Pergamon

Int. J. Solids Structures Vol. 31, No. 20, pp. 2793–2806, 1994

0020–7683/94 $7.00 + .00

0020–7683(94)E0061–Y

EFFECTS OF COORDINATE SYSTEM ON THE ACCURACY OF COROTATIONAL FORMULATION FOR BERNOULLI–EULER'S BEAM

MASASHI IURA
Department of Civil Engineering, Tokyo Denki University, Hatoyama, Hiki, Saitama 350-03, Japan

(*Received* 2 *October* 1993; *in revised form* 28 *March* 1994)

Abstract—The objective of this paper is to examine the effects of coordinate system on the accuracy of corotational formulation for planar Bernoulli–Euler's beam. The corotational formulation has often been introduced with a small strain assumption from the outset. A fundamental question, therefore, has been raised as to whether or not the numerical solutions obtained approach the solutions of a theory of finite strains with finite displacements. On the basis of the method proposed herein, a theoretical study for convergence of numerical solutions is made by comparing the approximated strains in the locally convected coordinates with the exact ones in the fixed global coordinates. Then the effects of locally convected coordinates on the accuracy of numerical solutions are discussed. Numerical examples are demonstrated to show the validity of the present theoretical results.

1. INTRODUCTION

In the finite element analysis for a large displacement problem of flexible beams, the total Lagrangian formulation together with the fixed global coordinates has been used [e.g. Crespo Da Silva (1988); Geradin and Cardona (1989); Iura and Hirashima (1985); Iura and Atluri (1988); Iwakuma (1990); Reissner (1972); Simo and Vu-Quoc (1986)]. In this formulation, even if the relative or elastic deformations of the body undergoing finite rigid displacements are small, a highly nonlinear beam theory is indispensable for simulating the motion of beams.

The use of the corotational formulation is motivated by the assumption of small strains of the body undergoing the finite rigid displacements. On the basis of this assumption, a linear theory or a higher-order theory has often been introduced in the locally convected coordinates to derive the relations between the internal forces and the corresponding deformations [e.g. Ai and Nishino (1980); Belytschko and Hseih (1973); Crisfield (1990); Goto *et al.* (1975); Goto *et al.* (1987); Hsiao and Hou (1987); Iura and Iwakuma (1992); Iwakuma *et al.* (1987); Jennings (1968); Maeda *et al.* (1974); Meek and Loganathan (1989); Oran (1973); Powell (1969); Saafan (1963); Simo and Vu-Quoc (1986); Song and Haug (1980); Tezcan (1968); Tezcan and Mahapatra (1969); Yang (1973); Yoshida *et al.* (1980); Wen and Rahimzadeh (1983)]. The numerical solutions obtained show that the corotational formulation is a powerful one for simulating a large displacement problem. Very few papers, however, have been published to show the accuracy of the corotational formulation from a theoretical point of view. Goto *et al.* (1987) have shown that the exact solutions of equilibrium equations, which are derived in the locally convected coordinates under a small strain assumption, approach the solutions obtained by a theory of small strains with finite displacements. Since a small strain assumption has been employed from the outset in the locally convected coordinates, the numerical solutions obtained by the corotational formulation have been expected to approach the solutions obtained by a theory of small strains with finite displacements.

In this paper, a new method is presented for the corotational formulation. On the basis of the present method, we investigate the accuracy of the corotational formulation for planar Bernoulli–Euler's beam. The study of accuracy is made by comparing the residual or unbalanced forces derived by the corotational formulation with those by the exact

theory. If the existing method is used for the study of accuracy, we must derive the explicit expressions for the residual forces. Thus the comparison will be tedious work. The advantage of using the present method is that the comparison is possible by simply deriving the explicit forms for the strain components. Then the effects of coordinate system on the accuracy of numerical solutions are discussed. The coordinate systems employed are the secant coordinates and the tangential coordinates. It seems to be evident that the convergence of numerical solutions obtained by the secant coordinates is faster than that by the tangential coordinates. A theoretical study, however, would be necessary to support the above conclusion. It is noted that the converged solutions, obtained by the corotational formulation under a small strain assumption, approach the solutions by a theory of finite strains with finite displacements as the number of elements increases. This conclusion is different from that of Goto *et al.* (1987). The numerical examples, analysed herein, for the finite strain problems show the validity of the present theoretical results.

2. FORMULATION

2.1. *Existing formulation*

We describe briefly an existing procedure for obtaining the numerical solutions with the use of the tangent stiffness method [see Oran (1973)]. The relations between the basic member forces $\{S\}$ and deformations $\{u\}$, referred to as the locally convected coordinates, are obtained as

$$\{S\} = \{S(u)\}. \tag{1}$$

The incremental relations are expressed from eqn (1) as

$$\{\Delta S\} = [t]\{\Delta u\}, \tag{2}$$

where $[t]$ is the local tangent stiffness matrix for relative deformations. The relations between the member end forces $\{F\}$ referred to the fixed global coordinates and the basic member forces $\{S\}$ are written as

$$\{F\} = [B]\{S\}, \tag{3}$$

where $[B]$ is the instantaneous static matrix. The incremental values of the basic member deformations $\{\Delta u\}$ are expressed, in terms of the incremental values of the member end displacements $\{\Delta v\}$ referred to the fixed global coodinates, as

$$\{\Delta u\} = [B]^{\mathrm{T}}\{\Delta v\}, \tag{4}$$

where the superscript T denotes transpose. The increment of $\{F\}$ is expressed, with the help of eqn (3), as

$$\{\Delta F\} = [\Delta B]\{S\} + [B]\{\Delta S\}. \tag{5}$$

By using the relation such that $[\Delta B]\{S\} = [g]\{\Delta v\}$ and eqns (2) and (4), we have

$$\begin{aligned}\{\Delta F\} &= ([B][t][B]^{\mathrm{T}} + [g])\{\Delta v\} \\ &= [T_{\mathrm{G}}]\{\Delta v\},\end{aligned} \tag{6}$$

where $[T_{\mathrm{G}}]$ is the global tangent stiffness matrix. Since the direct use of eqn (6) for obtaining the incremental solutions Δv leads to erroneous results, it is common to use the following iterative procedure [see Bathe (1982)]:

$$[T_G]^i_{N+1}\{\Delta v\}^i_N = \{\Delta R\}^i_{N+1}$$

$$\{\Delta R\}^i_{N+1} = \{F\}_{N+1} - [b(v)]^i_{N+1}\{S(v)\}^i_{N+1}, \tag{7}$$

where the subscript N denotes the load step, the superscript i the iteration counter and the vector $\{\Delta R\}$ is known as the residual or unbalanced force vector. The convergence rate of numerical solutions depends on the tangent stiffness matrix, while the accuracy of numerical solutions depends on the residual forces. Therefore, the explicit expressions for the residual forces are necessary for studying the accuracy of numerical solutions as long as the above method is employed.

2.2. *Present formulation*

The present formulation is briefly explained as follows. If the attention is confined to configuration-independent loads, the total potential energy for the beam may be expressed as

$$\Pi = \Pi_s + \Pi_f, \tag{8}$$

where Π_s is the strain energy function and Π_f the potential function for external forces. Let $\{u\}$ denote the displacement components referred to the locally convected coordinates. When the corotational formulation is employed, the strain energy function is expressed in terms of $\{u\}$ as

$$\Pi_s = \Pi_s(\{u\}). \tag{9}$$

From geometrical consideration, we will obtain the relationship between $\{u\}$ and the displacement components $\{v\}$ referred to the fixed global coordinates. This relationship may be expressed as

$$\{u\} = \{h(\{v\})\}, \tag{10}$$

where h is a nonlinear function of $\{v\}$. Substituting eqn (10) into eqn (9), we obtain the strain energy function which is expressed in terms of $\{v\}$ as

$$\Pi_s = \Pi_s(\{h(\{v\})\}). \tag{11}$$

Since the potential function Π_f for external forces can be expressed also in terms of $\{v\}$, the total potential energy is expressed in terms of $\{v\}$. Hence, following a standard procedure, we obtain the equilibrium equations of the beam element referred to the fixed global coordinates, expressed as

$$\left\{\frac{\partial \Pi}{\partial v_m}\right\} = 0, \tag{12}$$

where $\{v_m\}$ denotes the independent variables at each node. When the Newton–Raphson method is employed, the tangent stiffness matrix and the residual force vector are written as

$$[T_G] = \left[\frac{\partial^2 \Pi_s}{\partial v_m \partial v_n}\right], \quad \{\Delta R\} = -\left\{\frac{\partial \Pi}{\partial v_m}\right\}. \tag{13}$$

It is noted that the resulting global tangent stiffness matrix is always symmetric regardless of the magnitude of deformations.

Wen and Rahimzadeh (1983) have presented a similar formulation in which the tangent stiffness matrix and the residual force vector are expressed as

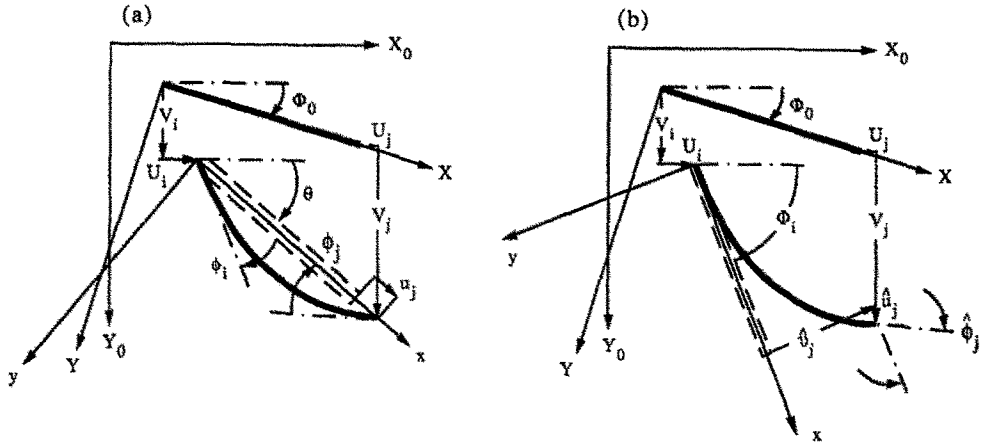

Fig. 1. Coordinate systems and beam kinematics; (a) secant coordinate system, (b) tangential coordinate system.

$$[T_G] = \left[\frac{\partial^2 \Pi^*}{\partial u_l \partial u_k}\frac{\partial u_l}{\partial v_m}\frac{\partial u_k}{\partial v_n} + \frac{\partial \Pi^*}{\partial u_k}\frac{\partial^2 u_k}{\partial v_m \partial v_n}\right]$$

$$\{\Delta R\} = -\left\{\frac{\partial \Pi^*}{\partial u_k}\frac{\partial u_k}{\partial v_m}\right\}, \tag{14}$$

where Π^* denotes the total potential energy which is the function of $\{u\}$ referred to the locally convected coordinates. From a mathematical point of view, eqn (14) is equivalent to eqn (13) as long as consistent formulation is employed. It is noted, however, that when the strain energy function or the kinematic relations between $\{u\}$ and $\{v\}$ are approximated, eqn (14) does not always lead to the same tangent stiffness matrix as that derived from eqn (13).

The advantage of using eqn (13) instead of eqn (14) becomes clear when the residual force vector derived by the corotational formulation is compared with that by the total Lagrangian method. If eqn (14) is used, the comparison becomes possible only when the explicit expressions for the residual force vector are given, though it is cumbersome to derive the residual force vector. When eqn (13) is used, on the other hand, the comparison is possible without deriving the explicit expressions for the residual force vector, but is easily carried out by simply deriving the explicit form for the potential energy. When the corotational formulation is used, the strain energy function is often approximated. It is enough, therefore, to compare the strain components derived by the corotational formulation with those by the total Lagrangian method.

3. BASIC EQUATIONS

There are a variety of choices to define the locally convected coordinates. Figure 1(a) shows the commonly used coordinate system, called the secant coordinate system, in which the end nodes of the element after the deformation are connected by the x axis. Figure 1(b) shows the coordinate system, called the tangential coordinate system, in which the x axis is taken as the tangent to the beam axis. In the latter coordinate system, no reciprocal of trigonometric functions appears to simulate the motion of planar beams undergoing finite rotations. Although there are other choices for the coordinate system, the above two coordinate systems are employed herein to investigate the effects of coordinate system on the accuracy of numerical solutions.

The strain energy function for Bernoulli–Euler's beam may be expressed as [e.g. Iwakuma (1990); Reissner (1972)]

$$\Pi_s = \int_0^l \left[\frac{EA}{2}(\varepsilon)^2 + \frac{EI}{2}(\kappa)^2 \right] dx, \tag{15}$$

where ε is the axial strain, κ the curvature, EA the axial stiffness, EI the flexual stiffness and l the length of the undeformed beam axis. The displacement components in the fixed global coordinates are denoted by $d_x = U$, $d_y = V$, $\lambda = \Phi$ and $\lambda_0 = \Phi_0$. In the locally convected coordinates, the displacement components are denoted by $d_x = u$, $d_y = v$, $\lambda = \phi$ and $\lambda_0 = 0$ for the secant coordinate system, and $d_x = \hat{u}$, $d_y = \hat{v}$, $\lambda = \hat{\phi}$ and $\lambda_0 = 0$ for the tangential coordinate system. The exact strain components are expressed in terms of the displacement components as (Reissner, 1972)

$$\begin{aligned} \varepsilon &= \{(d_x' + \cos\lambda_0)^2 + (d_y' + \sin\lambda_0)^2\}^{1/2} - 1 \\ \kappa &= \frac{d_y''(d_x' + \cos\lambda_0) - d_x''(d_y' + \sin\lambda_0)}{(d_x' + \cos\lambda_0)^2 + (d_y' + \sin\lambda_0)^2}, \end{aligned} \tag{16}$$

where $(\ )'$ denotes $d(\ )/dx$. According to Reissner (1972), the following kinematic relationships are obtained:

$$\begin{aligned} (1+\varepsilon)\sin\lambda &= d_y' + \sin\lambda_0 \\ (1+\varepsilon)\cos\lambda &= d_x' + \cos\lambda_0. \end{aligned} \tag{17}$$

In view of eqns (16) and (17), the strain components are rewritten as

$$\begin{aligned} \varepsilon &= (d_x' + \cos\lambda_0)\cos\lambda + (d_y' + \sin\lambda_0)\sin\lambda - 1 \\ \kappa &= (d_y''\cos\lambda - d_x''\sin\lambda)/(1+\varepsilon). \end{aligned} \tag{18}$$

Note that eqns (16)–(18) hold for both the fixed global and locally convected coordinates.

Let $(\ )_i$ and $(\ )_j$ denote the values at the nodes i and j of the beam element, respectively. According to the definition of the secant coordinate system, the non-zero values at the nodes i and j are ϕ_i, u_j and ϕ_j. The relationships between the nodal displacement components and the total displacement components are expressed as [see Fig. 1(a)]

$$\begin{Bmatrix} \phi_i \\ u_j \\ \phi_j \end{Bmatrix} = \begin{Bmatrix} \Phi_i - \theta \\ (U_j - U_i + l\cos\Phi_0)\cos\theta + (V_j - V_i + l\sin\Phi_0)\sin\theta - l \\ \Phi_j - \theta \end{Bmatrix}, \tag{19}$$

where

$$\begin{aligned} \cos\theta &= (U_j - U_i + l\cos\Phi_0)/(l+u_j) \\ \sin\theta &= (V_j - V_i + l\sin\Phi_0)/(l+u_j) \\ l + u_j &= [(U_j - U_i + l\cos\Phi_0)^2 + (V_j - V_i + l\sin\Phi_0)^2]^{1/2} \end{aligned} \tag{20}$$

and $\theta = \Phi - \phi$.

According to the definition of the tangential coordinate system, the non-zero values at the nodes i and j are $\hat{u}_j$, $\hat{v}_j$ and $\hat{\phi}_j$. Geometrical consideration leads to the following relationships [see Fig. 1(b)]:

$$\begin{Bmatrix} \hat{u}_j \\ \hat{v}_j \\ \hat{\phi}_j \end{Bmatrix} = \begin{bmatrix} \cos\Phi_i & \sin\Phi_i & 0 \\ -\sin\Phi_i & \cos\Phi_i & 0 \\ 0 & 0 & 1 \end{bmatrix} \begin{Bmatrix} U_j - U_i + l\cos\Phi_0 - l\cos\Phi_i \\ V_j - V_i + l\sin\Phi_0 - l\sin\Phi_i \\ \Phi_j - \Phi_i \end{Bmatrix}, \tag{21}$$

where $\Phi_i = \Phi - \hat{\phi}$. The relationships between Φ_i and the displacement components are obtained as

$$\cos\Phi_i = \frac{(U_j - U_i + l\cos\Phi_0)(l+\hat{u}_j) + (V_j - V_i + l\sin\Phi_0)\hat{v}_j}{(l+\hat{u}_j)^2 + (\hat{v}_j)^2}$$

$$\sin\Phi_i = \frac{(V_j - V_i + l\sin\Phi_0)(l+\hat{u}_j) - (U_j - U_i + l\cos\Phi_0)\hat{v}_j}{(l+\hat{u}_j)^2 + (\hat{v}_j)^2}. \tag{22}$$

For later convenience, we consider the shape functions which will be used for the finite element implementation. When the inconsistent shape functions are used, the strain components are not invariant under the transformation of coordinates. The conditions which yield the invariant strain components are expressed, with the help of eqn (18), as

$$\begin{aligned} U' + \cos\Phi_0 &= (u'+1)\cos\theta - v'\sin\theta \\ V' + \sin\Phi_0 &= (u'+1)\sin\theta + v'\cos\theta \end{aligned} \tag{23}$$

for the secant coordinate system and

$$\begin{aligned} U' + \cos\Phi_0 &= (\hat{u}'+1)\cos\Phi_i - \hat{v}'\sin\Phi_i \\ V' + \sin\Phi_0 &= (\hat{u}'+1)\sin\Phi_i + \hat{v}'\cos\Phi_i \end{aligned} \tag{24}$$

for the tangential coordinate system. It follows from eqns (23) and (24) that the order of d_x should be the same as that of d_y. Therefore, when a cubic polynomial is used to interpolate d_y, d_x must also be interpolated by a cubic polynominal. To determine the coefficient of shape functions, the kinematic relations expressed by eqns (17) should not be violated. The cubic shape functions which satisfy the kinematic relations are written as

$$\begin{aligned} d_x &= f_1 d_{xi} + f_2 d_{xj} + f_3\{(1+\varepsilon_i)\cos\lambda_i - \cos\lambda_0\} + f_4\{(1+\varepsilon_j)\cos\lambda_j - \cos\lambda_0\} \\ d_y &= f_1 d_{yi} + f_2 d_{yj} + f_3\{(1+\varepsilon_i)\sin\lambda_i - \sin\lambda_0\} + f_4\{(1+\varepsilon_j)\sin\lambda_j - \sin\lambda_0\}, \end{aligned} \tag{25}$$

where f_1 to f_4 are given by

$$\begin{aligned} f_1 &= 1 - \frac{3x^2}{l^2} + 2\frac{x^3}{l^3} \\ f_2 &= 3\frac{x^2}{l^2} - 2\frac{x^3}{l^3} \\ f_3 &= x - \frac{2x^2}{l} + \frac{x^3}{l^2} \\ f_4 &= -\frac{x^2}{l} + \frac{x^3}{l^2}. \end{aligned} \tag{26}$$

When the above shape functions are used, the axial strain ε at each node joins in the degrees of freedom in addition to d_x, d_y and λ. The increase of the number of degrees of freedom makes the element expensive. Furthermore, a special technique is needed for the transformation of ε. It is common, therefore, to use a linear shape function for u and $\hat{u}$ and a

cubic shape function for v and $\hat{v}$. The conventional shape functions used in the corotational formulation are expressed as

$$d_x = \left(1-\frac{x}{l}\right)d_{xi}+\frac{x}{l}d_{xj}$$

$$d_y = f_1 d_{yi}+f_2 d_{yj}+f_3\lambda_i+f_4\lambda_j. \tag{27}$$

It should be noted that the use of the conventional shape functions does not lead to the invariant strain components.

4. ACCURACY OF COROTATIONAL FORMULATION

In this section we consider the accuracy of corotational formulation in which a linear theory is introduced to describe the relative motion. It is well known that the accuracy of numerical results depends on the residual forces used. When the residual forces derived by the corotational formulation approach that by an exact theory, the resulting numerical solutions may approach those obtained by the exact theory. Therefore we will compare the residual forces in the locally convected coordinates with that derived by an exact theory in the fixed global coordinates. As shown in Section 2.2, as long as the present method is used, the explicit forms of the residual forces are unnecessary for the comparison of the residual forces. It is enough for the present study to compare the approximated strain in the locally convected coordinates with the exact ones in the fixed global coordinates.

In Section 4.1 we compare the linear strains in the secant coordinate system with the exact ones in the fixed global coordinate system. Comparison is made in Section 4.2 between the linear strains in the tangential coordinate system and the exact ones in the fixed global coodinate system. In what follows, for the sake of brevity, Φ_0 is taken as 0 without losing generality.

4.1. *Secant coordinate system*

In the secant coordinate system, a linear theory yields the relationships between the strain and displacement components, expressed as

$$\varepsilon_1 = u' = \frac{u_j}{l}$$

$$\kappa_1 = v'' = \left(-\frac{4}{l}+\frac{6x}{l^2}\right)\phi_i+\left(-\frac{2}{l}+\frac{6x}{l^2}\right)\phi_j, \tag{28}$$

where the conventional shape functions of eqn (27) are used.

First, we consider the accuracy of the axial strain. Substituting eqn (19) into eqn (28a), we have

$$\varepsilon_1 = \left(\frac{U_j-U_i}{l}+1\right)\cos\theta+\frac{(V_j-V_i)}{l}\sin\theta-1. \tag{29}$$

In view of eqns (20), (28) and (29), we obtain

$$(1+\varepsilon_1)^2 = \left(\frac{U_j-U_i}{l}+1\right)^2+\left(\frac{V_j-V_i}{l}\right)^2. \tag{30}$$

With the help of eqn (16a), the exact axial strain is written, in terms of the displacement components in the fixed global coordinates, as

$$(1+\varepsilon)^2 = (U'+1)^2+(V')^2. \tag{31}$$

When the forward difference is used to approximate U' and V', we have $U' = (U_j-U_i)/l$ and $V' = (V_j-V_i)/l$. Then we obtain $\varepsilon_1 = \varepsilon$. The accuracy of ε_1 is, therefore, the same as that of the forward difference; the accuracy of ε_1 is $O(l)$. The accuracy of the forward difference has been established [e.g. Atkinson (1978)]. It is expected, therefore, that ε_1 approaches ε as the number of elements increases.

Second, let us consider the accuracy of the curvature, the exact form of which is given by eqn (16b) or (18b). Since it is difficult to compare eqn (28b) with (16b) or (18b) directly, we introduce the consistent shape functions of eqns (25) into eqn (18b). Then we have

$$\kappa_c = \left(-\frac{4}{l}+\frac{6x}{l^2}\right)\frac{(1+\varepsilon_i)\sin(\phi_i-\phi)+(1+\varepsilon_1)\sin\phi}{1+\varepsilon} + \left(-\frac{2}{l}+\frac{6x}{l^2}\right)\frac{(1+\varepsilon_j)\sin(\phi_j-\phi)+(1+\varepsilon_1)\sin\phi}{1+\varepsilon}, \tag{32}$$

where the subscript c is used to show that the consistent shape functions are introduced into the exact relationship between strain and displacement components. As will be shown, the use of κ_c gives a satisfactory rate of convergence for the finite element solutions. Therefore, κ_c may be used as a precise curvature. As stated before, the neglect of the terms of order higher than $O(l^2)$ leads to $\varepsilon = \varepsilon_1$. In this case the axial strain becomes constant so that $\varepsilon = \varepsilon_i = \varepsilon_j$. Then the curvature κ_c takes the form

$$\kappa_c = \left(-\frac{4}{l}+\frac{6x}{l^2}\right)[\sin(\phi_i-\phi)+\sin\phi]+\left(-\frac{2}{l}+\frac{6x}{l^2}\right)[\sin(\phi_j-\phi)+\sin\phi]. \tag{33}$$

Since $\phi = \Phi-\theta$, we have

$$\sin\phi = \frac{1}{(1+\varepsilon)(1+\varepsilon_1)}\left[V'\left(\frac{U_j-U_i}{l}+1\right)-(U'+1)\left(\frac{V_j-V_i}{l}\right)\right]. \tag{34}$$

When the forward difference is used to interpolate U' and V', the right-hand side of eqn (34) becomes zero. Therefore, within the accuracy of $O(l^2)$, we may assume that $\sin\phi \approx \phi$. Since the order of ϕ_i and ϕ_j is the same as that of ϕ, we may have the relations that $\sin(\phi_j-\phi) \approx \phi_j-\phi$ and $\sin(\phi_i-\phi) \approx \phi_i-\phi$. Substituting these approximations into eqn (33) and comparing the resulting equation with eqn (28b), we have $\kappa_c = \kappa_1$.

When l becomes very small, the forward difference may lead to good approximation for U' and V'. Then we will have the relations that $\varepsilon_1 \approx \varepsilon$ and $\kappa_1 \approx \kappa_c$. Thus it is concluded that the numerical solutions obtained by ε_1 and κ_1 approach the solutions of the exact theory as the number of elements increases.

4.2. *Tangential coordinate system*

When the tangential coordinate system is used, a linear theory yields the relationships between the strain and displacement components, expressed as

$$\hat{\varepsilon}_1 = \hat{u}' = \frac{\hat{u}_j}{l}$$

$$\hat{\kappa}_1 = \hat{v}'' = \left(\frac{6}{l^2}-\frac{12x}{l^3}\right)\hat{v}_j+\left(-\frac{2}{l}+\frac{6x}{l^2}\right)\hat{\phi}_j, \tag{35}$$

where the conventional shape functions of eqn (27) are used. Substituting eqn (21) into eqn (35), we have

$$\hat{\varepsilon}_1 = \left(\frac{U_j - U_i}{l} + 1\right)\cos\Phi_i + \frac{(V_j - V_i)}{l}\sin\Phi_i - 1$$

$$\hat{\kappa}_1 = \left(\frac{6}{l^2} - \frac{12x}{l^3}\right)[(V_j - V_i)\cos\Phi_i - (U_j - U_i + l)\sin\Phi_i] - \left(\frac{2}{l} - \frac{6x}{l^2}\right)(\Phi_j - \Phi_i). \tag{36}$$

First, we consider the accuracy of $\hat{\varepsilon}_1$. Using eqns (22), (35a) and (36a), we obtain

$$(1+\hat{\varepsilon}_1)^2 = \left(\frac{U_j - U_i}{l} + 1\right)^2 + \left(\frac{V_j - V_i}{l}\right)^2 - \left(\frac{\hat{v}_j}{l}\right)^2. \tag{37}$$

When U' and V' are assumed to be evaluated correctly by the forward difference, it is found from eqns (31) and (37) that the last term on the right-hand side must vanish to yield $\hat{\varepsilon}_1 = \varepsilon$. This condition may be written in the following form:

$$\left(\frac{U_j - U_i}{l}\right)^2, \quad \left(\frac{V_j - V_i}{l}\right)^2 \gg \left(\frac{\hat{v}_j}{l}\right)^2. \tag{38}$$

Since $(U_j - U_i)/l$ or $(V_j - V_i)/l$ can be small, it is difficult to say whether or not the above relation holds. We consider, therefore, another estimation for the accuracy of $\hat{\varepsilon}_1$ which follows.

The exact axial strain is rewritten, with the help of eqns (18a) and (21), as

$$\varepsilon = \frac{1}{\cos\hat{\phi}}[(U'+1)\cos\Phi_i + V'\sin\Phi_i] - 1. \tag{39}$$

It follows from eqns (36a) and (39) that we have $\hat{\varepsilon}_1 \approx \varepsilon$ when the following approximations hold:

$$\cos\hat{\phi} \approx 1, \quad U' \approx (U_j - U_i)/l, \quad V' \approx (V_j - V_i)/l.$$

The last two approximations denote the forward difference of U' and V', while the first approximation holds when $1 \gg (\hat{\phi})^2$. By expanding Φ into Taylor's series at Φ_i, we have

$$\Phi = \Phi_i + x\Phi_i' + O(x^2).$$

Since $\hat{\phi} = \Phi - \Phi_i = x\Phi_i' + O(x^2)$, the relation $1 \gg (\hat{\phi})^2$ holds when the second-order term of Taylor's series of Φ is assumed to be small. This assumption may hold as the number of elements increases, yet is more strict than that used in the forward difference. Therefore, in order to obtain $\hat{\varepsilon}_1 \approx \varepsilon$, we need a more strict condition than that used to obtain $\varepsilon_1 \approx \varepsilon$; the rate of convergence for $\hat{\varepsilon}_1$ is slower than that for ε_1.

Second, we consider the accuracy of $\hat{\kappa}_1$. It is difficult again to compare eqn (36b) with (16b) or (18b) directly. We introduce, therefore, the consistent shape functions of eqn (25) into eqn (18b), and obtain

$$\kappa_c = \left(\frac{6}{l^2} - \frac{12x}{l^3}\right)[(V_j - V_i)\cos\Phi_i - (U_j - U_i + l)\sin\Phi_i]\frac{\cos\hat{\phi}}{1+\varepsilon}$$
$$+ \left(-\frac{2}{l} + \frac{6x}{l^2}\right)\left[\frac{1+\varepsilon_j}{1+\varepsilon}\sin(\Phi_j - \Phi) + \frac{1+\hat{\varepsilon}_1}{1+\varepsilon}\sin(\Phi - \Phi_i)\right] + \left(-\frac{4}{l} + \frac{6x}{l^2}\right)\left(\frac{\hat{\varepsilon}_1 - \varepsilon_i}{1+\varepsilon}\right)\sin\hat{\phi}. \tag{40}$$

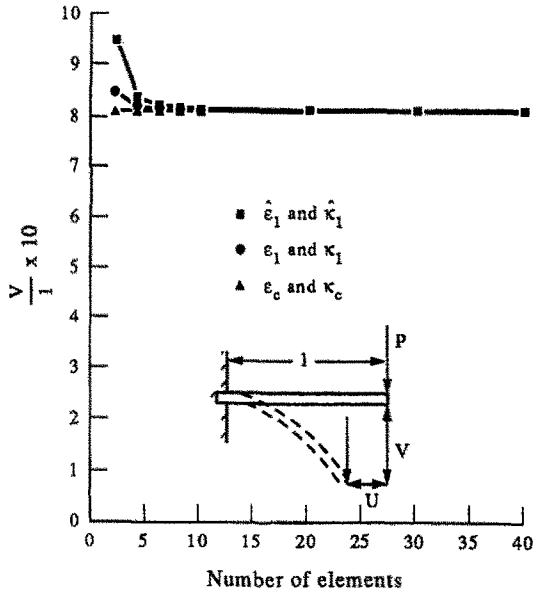

Fig. 2. Convergence of FE solutions of a cantilever beam subjected to end force.

Let us assume that $\varepsilon \approx \hat{\varepsilon}_1$ holds. Then the axial strain becomes constant so that we obtain $\varepsilon \approx \hat{\varepsilon}_1 \approx \varepsilon_i \approx \varepsilon_j$. Thus the curvature κ_c takes the form

$$\kappa_c = \left(\frac{6}{l^2} - \frac{12x}{l^3}\right)[(V_j - V_i)\cos\Phi_i - (U_j - U_i + l)\sin\Phi_i]\frac{\cos\hat{\phi}}{1+\varepsilon} - \left(\frac{2}{l} - \frac{6x}{l^2}\right)[\sin(\Phi_j - \Phi) + \sin(\Phi - \Phi_i)]. \quad (41)$$

It follows from eqns (36b) and (41) that the following assumptions in addition to $\varepsilon \approx \hat{\varepsilon}_1$ should hold to yield $\hat{\kappa}_1 \approx \kappa_c$:

$$\frac{\cos\hat{\phi}}{1+\varepsilon} \approx 1, \quad \sin(\Phi_j - \Phi) \approx \Phi_j - \Phi, \quad \sin(\Phi - \Phi_i) \approx \Phi - \Phi_i (= \hat{\phi}).$$

Since the order of Φ_j is the same as that of Φ_i, the order of $\Phi_j - \Phi$ is the same as that of $\hat{\phi}$. The last two approximations, therefore, may hold when $1 \gg (\hat{\phi})^2$. In order to satisfy the first approximation, a small axial strain assumption in addition to $1 \gg (\hat{\phi})^2$ must be introduced. From a theoretical point of view, therefore $\hat{\kappa}_1$ does not approach κ_c when the axial strain cannot be neglected in comparison with unity. In most of the problems, however, the order of ε is O $(10^{-2} \sim 10^{-1})$ at the most. In this case, $\hat{\kappa}_1$ will approach κ_c as the number of elements increases. According to the numerical experiments, the solutions obtained by $\hat{\varepsilon}_1$ and $\hat{\kappa}_1$ approach the exact solutions of a finite strain theory even in the finite strain problems. The rate of convergence for those numerical solutions is slower than that obtained by ε_1 and κ_1.

5. NUMERICAL EXAMPLES

Several numerical examples are considered in this section to confirm the theoretical results discussed above. The strain energy function is integrated exactly except for ε_c and κ_c in which the numerical integration method is used. The full Newton–Raphson method is used with the arc length method. The iteration is terminated if the Euclidean norm of the unbalanced forces is less than the prescribed value.

5.1. *Cantilever subjected to vertical force*

As the first example, we consider the cantilever beam subjected to the end force, as shown in Fig. 2. The slenderness ratio of the beam is taken as 100. The converging processes

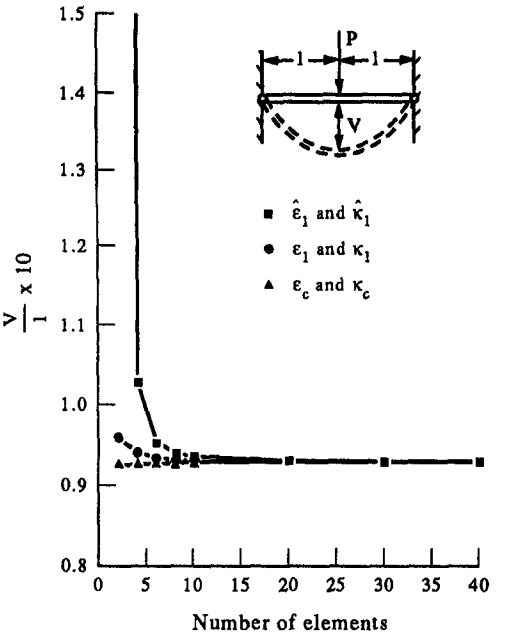

Fig. 3. Convergence of FE solutions of a beam with hinged ends.

of the finite element solutions for end deflections of the beam with $Pl^2/EI = 10.0$ are shown in Fig. 2. The numerical solutions obtained by ε_c and κ_c show excellent accuracy. These strain components, therefore, may be regarded as precise ones. As expected, the convergence rate of numerical solutions obtained by $\hat{\varepsilon}_1$ and $\hat{\kappa}_1$ is slower than that by ε_1 and κ_1. It should be noted that all of the numerical solutions approach the exact solution as the number of elements increases.

5.2. *Beam with hinged ends*

The second example is the beam with hinged ends, as shown in Fig. 3. The concentrated force is applied at the center of the beam. The slenderness ratio of the beam is 100. Because of symmetry only half is discretized. The converging processes of the finite element solutions for center deflection of the beam with $Pl^2/EI = 10.0$ are shown in Fig. 3. The converged solutions coincide with exact solutions obtained by Goto *et al.* (1990). The accuracy of the numerical solutions obtained by ε_c and κ_c is again satisfactory. The convergence rate of the numerical solutions obtained by $\hat{\varepsilon}_1$ and $\hat{\kappa}_1$ is very slow in this example. It should be noted once again that all of the numerical solutions approach the exact solution as the number of elements increases.

The third example is the same as the second one except that the slenderness ratio of the beam is 5. It is pointed out by Goto *et al.* (1990) that the difference between the numerical solutions obtained by the finite strain theory and those by the small strain theory does not appear remarkably when the slenderness ratio of the beam is higher than 10. A comparison between the analytical solutions obtained by both the finite strain theory and the small strain theory, and the present numerical solutions is made in Fig. 4. The solid line indicates the solutions of the finite strain theory and the dashed line the solution of the small strain theory. The present numerical solutions are obtained by using 40 elements. In this case all of the finite element solutions converge to the same value within four digits. It is noted that the converged solutions coincide with the solutions obtained by the finite strain theory not by the small strain theory. This fact agrees with the present theoretical conclusion.

5.3. *Cantilever subjected to axial force*

In the final example, we consider the cantilever beam subjected to an increasing compressive end force together with a small end moment, as shown in Fig. 5. The slenderness

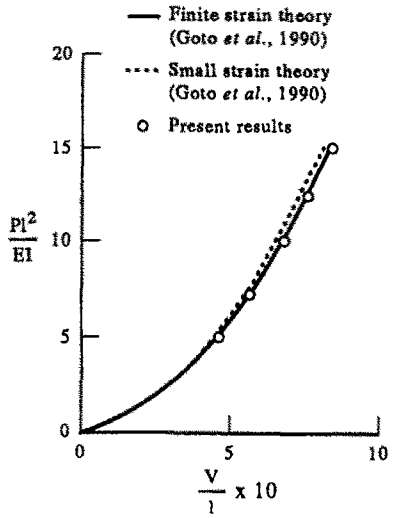

Fig. 4. Comparison between analytical and converged solutions for a beam with hinged ends.

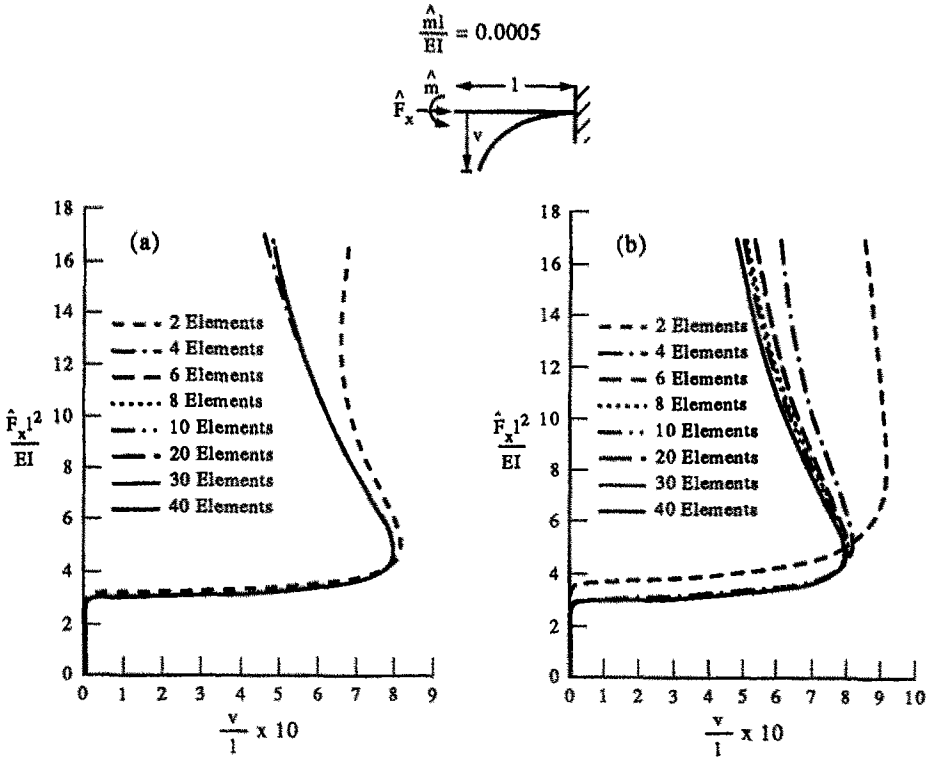

Fig. 5. Convergence of FE solutions of a cantilever beam subjected to axial force; (a) solutions by ε_1 and κ_1, (b) solutions by $\hat{\varepsilon}_1$ and $\hat{\kappa}_1$.

ratio of the beam is 4. In this model, there exists an obvious difference between the solutions obtained by the finite strain theory and those by the small strain theory. According to Goto *et al.* (1990), the buckling load derived by the finite strain theory is $\hat{F}_x l^2/EI = 3.048$ while that by the small strain theory is $\hat{F}_x l^2/EI = 2.467$. The converging processes of the solutions obtained by ε_1 and κ_1, and $\hat{\varepsilon}_1$ and $\hat{\kappa}_1$ are shown in Figs 5(a) and 5(b), respectively. When the small numbers of elements are used, the numerical results are not satisfactory especially in the range of the post-buckling. The buckling load, however, can be obtained precisely by using the small numbers of elements when ε_1 and κ_1 are employed. A comparison between the analytical solutions obtained by both the finite strain theory and the small

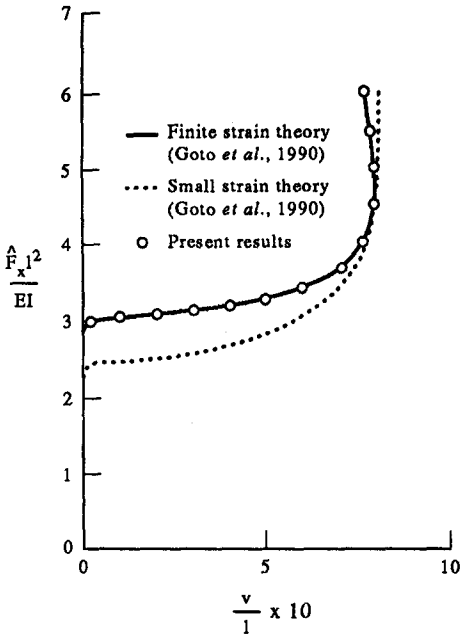

Fig. 6. Comparison between analytical and converged solutions for a cantilever beam subjected to axial force.

strain theory, and the converged solutions is made in Fig. 6. The solid line indicates the solutions of the finite strain theory and the dashed line the solution of the small strain theory. The converged solutions are obtained by using 40 elements so that all of the finite element solutions converge to the same value within four digits. It is shown that the converged solutions coincide with the solutions obtained by the finite strain theory not by the small strain theory. This numerical result shows once again the validity of the present theoretical study.

6. CONCLUDING REMARKS

The accuracy of the corotational formulation for planar Bernoulli–Euler's beam has been studied on the basis of the method proposed herein. The accuracy of numerical solutions depends on the residual forces used. Therefore comparison between the residual forces obtained by the corotational formulation and the exact one has been made. This comparison is possible without deriving the explicit forms of the residual forces. It is shown that the comparison between the approximated strains in the locally convected coordinates and the exact strains in the fixed global coordinates is enough to study the accuracy of the corotational formulation. Although a small strain assumption is used from the outset in the corotational formulation, the nonlinear terms are included in the transformation of coordinate system. These nonlinear terms play an important role in improving the accuracy of numerical solutions.

The effects of the local coordinate system on the accuracy of numerical solutions have been discussed. In the case of using the secant coordinate system, the accuracy of the corotational formulation is the same as that of the forward difference. It has been concluded that the numerical solutions obtained by the corotational formulation approach the solutions by a theory of finite strains with finite displacements as the number of elements increases. This conclusion disagrees with earlier conclusions derived by Goto *et al.* (1987). The numerical examples show the validity of the present theoretical results.

Acknowledgement—The author would like to thank the reviewers for their useful comments.

REFERENCES

Ai, M. and Nishino, H. (1980). Mechanics in geometrically nonlinear problem of discrete system and application to plane frame-works. *Proc. JSCE* **304,** 17–32 (in Japanese).

Bathe, K.-J. (1982). *Finite Element Procedures in Engineering Analysis*. Prentice-Hall, New York.

Belytschko, T. and Hseih, J. (1973). Non-linear transient finite element analysis with convected coordinates. *Int. J. Numer. Meth. Engng* **7,** 255–271.

Crespo Da Silva, M. R. M. (1988). Non-linear flexural–flexural–torsional–extensional dynamics of beams—1. Formulation. *Int. J. Solids Structures* **24**(12), 1225–1234.

Crisfield, M. A. (1990). A consistent co-rotational formulation for nonlinear, three-dimensional beam-elements. *Comput. Meth. Appl. Mech. Engng* **81,** 131–150.

Geradin, M. and Cardona, A. (1989). Kinematics and dynamics of rigid and flexible mechanisms using finite elements and quaternion algebra. *Comput. Mech.* **4**(2), 115–136.

Goto, S., Hane, G. and Tanaka, T. (1975). Tangent stiffness method for large deformation analysis of frame structure. *Proc. JSCE* **238,** 31–42 (in Japanese).

Goto, Y., Kasugai, T. and Nishino, F. (1987). On the choice of local moving coordinates in the finite displacement analysis of planar frames. *Proc. JSCE* **386**(8), 311–320.

Goto, Y., Yoshimitsu, T. and Obata, M. (1990). Elliptic integral solutions of plane elastica with axial and shear deformations. *Int. J. Solids Structures* **26**(4), 375–390.

Hsiao, K. M. and Hou, F. Y. (1987). Nonlinear finite element analysis of elastic frames. *Comput. Struct.* **26**(4), 693–701.

Iura, M. and Atluri, S. N. (1988). Dynamic analysis of finitely stretched and rotated three-dimensional space-curved beams. *Comput. Struct.* **29**(5), 875–889.

Iura, M. and Hirashima, M. (1985). Geometrically nonlinear theory of naturally curved and twisted rods with finite rotations. *Proc. JSCE* **362**(4), 107–117.

Iura, M. and Iwakuma, T. (1992). Dynamic analysis of the planar Timoshenko beam with finite displacement. *Comput. Struct.* **45**(1), 173–179.

Iwakuma, T. (1990). Timoshenko beam theory with extension effect and its stiffness equation for finite rotation. *Comput. Struct.* **34**(2), 239–250.

Iwakuma, T., Hasegawa, A., Nishino, F. and Kuranishi, S. (1987). Principle and numerical check of a stiffness equation for plane frames. *Proc. JSCE* **380**(7), 99–109.

Jennings, A. (1968). Frame analysis including change of geometry. *J. Struct. Div. ASCE* **94**(ST3), 627–644.

Maeda, Y., Hayashi, M. and Nakamura, M. (1974). An acceleration approach for large deformation structural analysis by incremental method. *Proc. JSCE* **223,** 1–9 (in Japanese).

Meek, J. L. and Loganathan, S. (1989). Large displacement analysis of space-frame structures. *Comput. Meth. Appl. Mech. Engng* **72,** 57–75.

Oran, C. (1973). Tangent stiffness in plane frames. *J. Struct. Div. ASCE* **99**(ST6), 973–985.

Powell, G. H. (1969). Theory of nonlinear elastic structures. *J. Struct. Div. ASCE* **95**(ST12), 2687–2701.

Reissner, E. (1972). On one-dimensional finite-strain beam theory: the plane problem. *J. Appl. Math. Phys.* **23,** 795–804.

Saafan, S. A. (1963). Nonlinear behavior of structural plane frames. *J. Struct. Div. ASCE* **89**(ST4), 557–579.

Simo, J. C. and Vu-Quoc, L. (1986). On the dynamics of flexible beams under large overall motions—The plane case: part 1. *J. Appl. Mech. ASME* **53,** 849–858.

Song, J. O. and Haug, E. J. (1980). Dynamic analysis of planar flexible mechanisms. *Comput. Meth. Appl. Mech. Engng* **24,** 359–381.

Tezcan, S. S. (1968). Discussion of "Numerical solution of nonlinear structures", by T. J. Poskitt. *J. Struct. Div. ASCE* **94**(ST6), 1613–1623.

Tezcan, S. S. and Mahapatra, B. C. (1969). Discussion of "Nonlinear analysis of elastic framed structures", by J. J. Connor, Jr, R. D. Logcher and S. C. Chan. *J. Struct. Div. ASCE* **95**(ST3), 519–523.

Yang, T. Y. (1973). Matrix displacement solution to elastica problems of beams and frames. *Int. J. Solids Structures* **9,** 829–842.

Yoshida, Y., Masuda, N., Morimoto, T. and Hirosawa, N. (1980). An incremental formulation for computer analysis of space framed structures. *Proc. JSCE* **300,** 21–31 (in Japanese).

Wen, R. K. and Rahimzadeh, J. (1983). Nonlinear elastic frame analysis by finite element. *J. Struct. Engng ASCE* **109,** 1952–1971.